1394–1399 Nucleic Acids Research Vol. 22, No. 8

Contacts between the growing peptide chain and the 23S RNA in the 50S ribosomal subunit

Katrin Stade, Sören Riens, Dmitry Bochkariov[1] and Richard Brimacombe*
Max-Planck-Institut für Molekulare Genetik, Abteilung Wittmann, Ihnestrasse 73, D-14195 Berlin, Germany and [1]Institute for Protein Research, Russian Academy of Science, Pushchino, Moscow Region 142292, Russia

Received January 25, 1994; Revised and Accepted March 11, 1994

ABSTRACT

Peptides of defined length carrying a diazirine photo-affinity label attached either to the α-NH_2 group of the N-terminal methionine residue, or to the ϵ-NH_2 group of an immediately adjacent lysine residue, were prepared *in situ* on *Escherichia coli* ribosomes in the presence of a synthetic mRNA analogue. Peptide growth was stopped simply by withholding the aminoacyl-tRNA cognate to an appropriate downstream codon. After photo-activation at 350 nm the sites of cross-linking to ribosomal RNA were determined by our standard procedures; the C-terminal amino acid of each peptide was labelled with tritium, in order to confirm whether the individual cross-linked complexes contained the expected 'full-length' peptide, as opposed to shorter products. The shortest peptides became cross-linked to sites within the 'peptidyl transferase ring' of the 23S RNA, namely to positions 2062, 2506, 2585 and 2609. However, already when the peptide was three or four residues long, a new cross-link was observed several hundred nucleotides away in another secondary structural domain; this site, at position 1781, lies within one of several RNA regions which have been implicated in other studies as being located close to the peptidyl transferase ring. Further application of this approach, combined with model-building studies, should enable the path of the nascent peptide through the large ribosomal subunit to be definitively mapped.

INTRODUCTION

It is generally accepted that the peptidyl transferase centre is located at the base of the central protuberance of the 50S ribosomal subunit, on the side facing the 30S subunit (1,2). However, the nascent protein appears to leave the ribosome from a site almost diametrically opposite, at the base of the 50S subunit on the solvent side (3). The important question as to how the growing peptide progresses between these two sites has not yet been solved. Yonath *et al.* (4) have proposed that the peptide passes through the 'tunnel' which they observed in three-dimensional reconstructions of the 50S subunit, but other authors (5) prefer the concept of a 'channel' on the subunit surface. One obvious approach to investigate this problem is to make a systematic 'site-directed' cross-linking study, using a defined set of peptides carrying an affinity label at or near to their N-terminus. Such a study was undertaken some time ago by Cantor *et al.* (6), but their experiments had the dual disadvantages that the peptide analogues were not synthesized *in situ* on the ribosome (and may therefore have failed to become correctly located in the channel or tunnel), and that their study was at that time limited to an analysis of the cross-linked ribosomal proteins.

The recent observation (7) that the region of the peptidyl transferase centre is rich in RNA, together with the possibility that the peptidyl transferase activity itself is mediated by the RNA (8), have prompted us to start a new 'RNA-oriented' investigation into the path of the nascent peptide, using affinity-labelled peptides biosynthesized *in situ* on the ribosome and taking advantage of techniques recently developed in our laboratory (9–11) for the analysis of cross-link sites at nucleotide resolution on the large ribosomal RNA molecules. The affinity reagent which we have chosen for this purpose is the N-hydroxysuccinimide ester of 4-(3-trifluoromethyl diazirino)-benzoic acid (12, cf. 13). Such diazirine derivatives have been successfully applied in a number of cross-linking studies with proteins or peptides (e.g. 14,15), and have the advantage that they can be photoactivated at 350 nm (13); since the ribosome is 'transparent' at this wavelength, it should be possible for the affinity-labelled peptides to form cross-links even when the label is deeply buried in the 50S subunit. Here we present the first results of our cross-linking analyses using this approach, with peptides up to four amino acids in length.

MATERIALS AND METHODS

Preparation of mRNA, and tRNA derivatives

An mRNA analogue was prepared by T7 transcription from a synthetic DNA template (9,11). This mRNA had the sequence GGG AGA AAG AAA AUG AAA UUC GAA CUG GAC ACC, carrying codons for methionine, lysine, phenylalanine and glutamic acid (M, K, F, E, underlined). Individual tRNA species

*To whom correspondence should be addressed

(Subriden RNA, USA) were charged with the appropriate amino acids, using tRNA-free S-150 enzymes (16). Met-tRNA^{fMet} was either formylated, or derivatized at the α-NH_2 group with the diazirine reagent (12), as described in ref. 11. Lys-tRNA^{Lys} was specifically derivatized at the ϵ-NH_2 group, as described by Görlich *et al.* (17). The peptides were labelled in one of two ways: (a) The methionine was labelled with ^{35}S at high specific activity (500,000 cpm/pmol), so as to obtain strong autoradiograms on polyacrylamide gels (see below) of the cross-linked products, or (b) the methionine was ^{35}S-labelled at lower specific activity (50,000 cpm/pmol), and at the same time the C-terminal amino acid of the peptide under study was labelled with ^{3}H (to a specific activity of 50,000−100,000 cpm/pmol) in order to be able to test for the presence of the full-length peptide in the individual cross-linked products.

Biosynthesis of peptides

100 μl reaction mixtures were prepared containing 100 pmol of 70S 'tight couple' *E.coli* ribosomes (16), 150 pmol formylated or diazirine-derivatized Met-tRNA^{fMet}, 500 pmol mRNA (see above), and 100 pmol each of IF-1, IF-2 and IF-3 (a generous gift from Dr C.Gualerzi) in 20 mM HEPES−KOH pH 7.5, 60 mM NH_4Cl, 7.5 mM $Mg(OAc)_2$, 1 mM dithiothreitol and 1 mM GTP (pH 7.5). The mixtures were incubated for 10 min at 37°C. Next, 100 μl reactions were prepared containing 200 pmol of each of the charged tRNA species required for the particular peptide, EF-Tu (18) in a 2-fold molar excess over the total charged tRNAs, and 100 pmol of EF-G (18), in 20 mM HEPES−KOH pH 7.5, 60 mM NH_4Cl, 13 mM $Mg(OAc)_2$, 1 mM dithiothreitol and 0.1 mM GTP. After 2 min at 37°C each mixture was added to the initiation complex just described (total volume 200 μl), and incubated for a further 15 min at 37°. The reaction mixtures were then placed on ice and irradiated at 350 nm for 10 min (19). Control reactions were prepared in which the diazirine-derivatized Met-tRNA^{fMet} or Lys-tRNA^{Lys} was subjected additionally to this same irradiation procedure (to destroy the diazirino group) before the incubation with ribosomes. Puromycin tests were performed as described by Rheinberger *et al.* (16).

Isolation of cross-linked products and analysis of sites of cross-linking on the 23S RNA

The ribosomal RNA cross-linked to peptidyl tRNA was isolated from the irradiated ribosomal complexes by a series of sucrose gradient centrifugations, as described by Stade *et al.* (9), with the exception that instead of the final sucrose gradient in SDS to separate RNA from ribosomal protein, a phenol extraction was made. Cross-linking was exclusively to the 23S RNA, typical yields being of the order of 250,000 cpm of ^{35}S-radioactivity (from experiments made with methionine at the higher specific activity). The sites of cross-linking on the RNA were first localized by ribonuclease H digestion (9,11) in the presence of pairs of oligodeoxynucleotides complementary to selected regions of the 23S sequence. 10- or 15-mer oligonucleotides were used for this purpose, and in the text and Figure legends the 23S RNA positions complementary to the central residue of each oligonucleotide are given. The ribonuclease H digestion products were separated on 5% polyacrylamide gels, and the ^{35}S-methionine radioactivity was visualized by fluorography as in ref. 11. In experiments where ^{3}H-labelled C-terminal amino acids had been incorporated together with low specific activity ^{35}S-methionine (see above), appropriate bands were cut out from the dried ribonuclease H gels, soaked for 2 hr in 200 μl H_2O, then shaken overnight in 10 ml of a toluene scintillation fluid containing 0.4% PPO and 8% v/v Soluene 350 (Packard), prior to counting; typical radioactivity values in the gel bands were of the order of 100−1000 cpm each for ^{3}H and ^{35}S.

After each cross-linked region within the 23S RNA had been 'narrowed down' as far as possible by a series of ribonuclease H digestions, the cross-link sites within these regions were localized further by the primer extension method (20,11), using samples prepared with pre-irradiated tRNA (see above) as controls.

RESULTS AND DISCUSSION

Peptides were biosynthesized on *E.coli* ribosomes in the presence of an mRNA analogue including a sequence coding for Met−Lys−Phe−Glu (M−K−F−E), together with the appropriate aminoacyl-tRNA species, as described in Materials and Methods. The diazirine reagent was attached either to the α-amino group of the N-terminal methionine (which we denote by M*) or to the ϵ-amino group (17) of the adjacent lysine (denoted by K*). In the latter case the peptides were N-formylated, thus enabling us to make parallel experiments with peptides carrying either an N-terminal diazirine group or the natural N-formyl group.

The N-terminal methionine residue was labelled with ^{35}S, and peptide growth was controlled by supplying only those aminoacyl-tRNA species required for the peptide being studied. In order to test whether the expected product had indeed been synthesized, experiments were made in which—in addition to the ^{35}S-labelled methionine—the C-terminal amino acid was ^{3}H-labelled (see Materials and Methods). Subsequently, the ^{3}H:^{35}S ratio in each individual cross-linked complex was measured (see below), the presence of tritium providing a simple but unambiguous proof that the corresponding full-length peptide was involved in the cross-link. Control experiments with tri- or tetrapeptides in which an 'intervening' non-radioactive aminoacyl-tRNA species was omitted showed no incorporation of ^{3}H-radioactivity into the cross-linked products.

After photo-activation of the ribosome−mRNA−peptidyl-tRNA complexes by irradiation at 350 nm (19), the 23S RNA cross-linked to peptidyl-tRNA was isolated by a series of sucrose gradients (9), followed by phenol extraction. From the radioactivity associated with the 70S ribosomes in the first sucrose gradient, it was estimated that in a typical experiment ca 20% of the ribosomes had participated in full-length peptide synthesis. Corresponding measurements of the radioactivity remaining associated with the 23S RNA after the final phenol extraction indicated that 2−4% of the bound peptide material became cross-linked. The cross-linking was always exclusively to 23S RNA (not to 16S RNA), and in control experiments with pre-irradiated tRNA (where the diazirine moiety in the aminoacyl-tRNA had been destroyed prior to the incubation with ribosomes; see Materials and Methods) the amount of radioactivity remaining associated with the 23S RNA was reduced by a factor of ten. The relatively low level of cross-linking observed is typical for a diazirine compound (cf. 14,15); the carbene radical generated by photo-activation of this type of reagent is extremely short-lived and highly reactive (21), which results in a rapid reaction with the solvent. On the other hand, the high reactivity has the advantage in a study of this type that the carbene takes an 'instantaneous snapshot' of its environment, rather than seeking

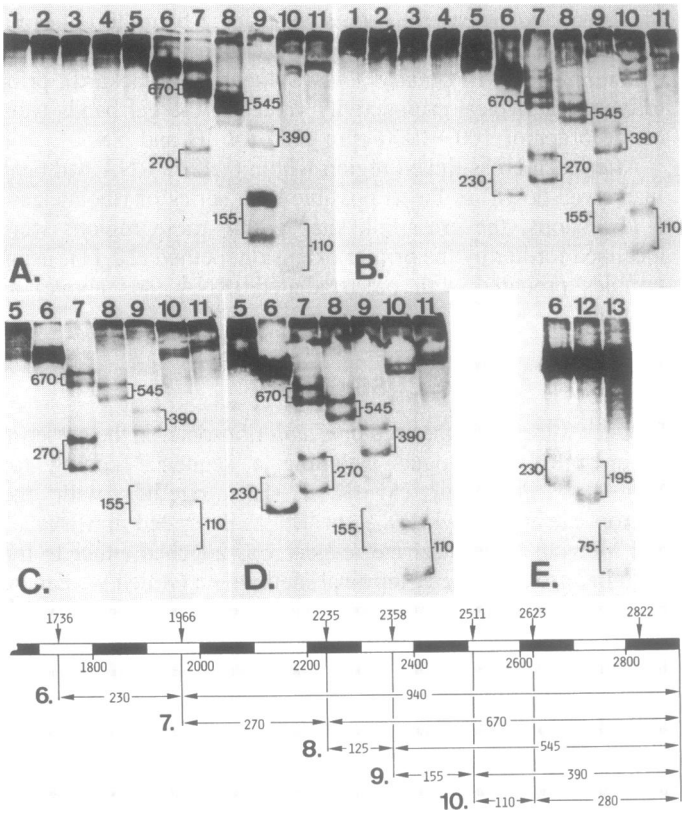

Figure 1. Ribonuclease H digests of cross-linked peptidyl-tRNA/23S RNA complexes, on 5% polyacrylamide gels (10). Panel **A** shows digests derived from a complex containing the simplest 'peptide' M*, panel **B** digests from a complex with the peptide M*KFE, panel **C** from the peptide MK*, and panel **D** from the peptide MK*FE. In each case the digestions were performed in the presence of pairs of oligodeoxynucleotides complementary to sequences centred on 23S positions 250/495 (lane 1), 495/780 (lane 2), 780/1045 (lane 3), 1045/1366 (lane 4), 1366/1736 (lane 5), 1736/1966 (lane 6), 1966/2235 (lane 7), 2235/2358 (lane 8), 2358/2511 (lane 9), 2511/2623 (lane 10) and 2623/2822 (lane 11). The approximate lengths of the 23S RNA fragments in each doublet band (see text) are indicated, and the locations of these fragments within the 3'-proximal half of the 23S RNA are shown schematically in the lower part of the Figure, arranged according to lane numbers 6 to 10. Panel **E** shows further digests of the complex from the peptide M*KFE to illustrate the progressive localization of the cross-link in lane 6 (panel B); here the additional lanes 12 and 13 were with oligodeoxynucleotides complementary to positions 1771/1966 (giving a 195-nucleotide fragment) and 1771/1845 (giving a 75-nucleotide fragment), respectively.

Table 1. Test for the presence of the full-length peptides M*KF and M*KFE, respectively, in the cross-linked complexes.

Cross-linked region and peptide		Radioactivity values			Normalised 3H:35S ratio
		^{3}H	^{35}S	^{3}H:^{35}S	
I	M*KF	580	584	1.0	0.6
	M*KFE	558	976	0.6	0.8
II	M*KF	297	720	0.4	0.2
	M*KFE	158	752	0.2	0.3
III	M*KF	62	106	0.6	0.4
	M*KFE	19	131	0.1	0.1
IV	M*KF	166	97	1.7	1.0
	M*KFE	117	163	0.7	1.0
V	M*KF[b]	–	–	–	–
	M*KFE	213	351	0.6	0.8

The Table shows the ^{3}H- and ^{35}S-radioactivities in the ribonuclease H gel bands (cf. Figure 1) corresponding to each of the cross-linked 23S RNA regions I to V (see Materials and Methods), and the ^{3}H:^{35}S radioactivity ratios. In the last column the individual ^{3}H:^{35}S ratios are normalized to the input specific activities of the amino acids[a]; a ratio of 1.0 thus indicates 100% full-length peptide, and a ratio of 0.0 denotes the absence of any full-length peptide.

[a]Input specific activities were 67,000 cpm/pmol (^{35}S–Met), 111,000 cpm/pmol (^{3}H–Phe) and 48,000 cpm/pmol (^{3}H–Glu), giving an expected ^{3}H:^{35}S ratio of 1.66 for M*KF (with C-terminal ^{3}H–Phe) and 0.72 for M*KFE (with C-terminal ^{3}H–Glu).

[b]Cross-link V in this case was too weak for a radioactive analysis.

a preferred cross-linking partner as is the case with longer-lived radicals.

The regions of the 23S RNA involved in cross-links to the various diazirine-derivatized peptides were determined by digestion with ribonuclease H in the presence of pairs of oligodeoxynucleotides complementary to selected sequences in the 23S molecule (9–11). Short 23S RNA fragments carrying ^{35}S-peptide radioactivity are only observed in the subsequent gel electrophoresis in those cases where the two oligodeoxynucleotides have 'straddled' a cross-link site. Examples are given in Figure 1. Panel A, from the simplest 'peptide' M*, shows no cross-linking in the 5'-region of the 23S RNA (lanes 1–6), but a 270-nucleotide fragment can be seen in lane 7, indicating a cross-link from the methionyl residue to the RNA between positions 1966–2235 (these positions corresponding to the central residues of the oligodeoxynucleotides used in the ribonuclease H digestion). Doublet bands are always observed in these experiments, because the tRNA is partially released from the cross-linked complex by hydrolysis of the ester bond during the 55°C incubation with ribonuclease H (11). The presence of a strongly radioactive 670-nucleotide band in lane 7 of panel A (Figure 1) shows that other cross-links must be present further towards the 3'-end of the 23S RNA, and these are resolved into a strong cross-link between positions 2358–2511 (the 155-nucleotide band in lane 9) and a weaker one between positions 2511–2623 (the 110-nucleotide band in lane 10). On the other hand, no band is seen in lane 8 corresponding to a cross-link between positions 2235 and 2358.

Panel B (Figure 1) shows the corresponding data from the tetrapeptide M*KFE. Here, the most important feature is the appearance of a new band, namely the 230-nucleotide fragment in lane 6, indicative of a cross-link lying between RNA positions 1736–1966. Furthermore, in comparison to panel A, the 110-nucleotide band (lane 10) has become stronger, whereas the 155-nucleotide band (lane 9) has become considerably weaker. As outlined in Materials and Methods, experiments were made with each peptide both at high ^{35}S-methionine specific activity (so as to obtain strong autoradiograms, as in Figure 1), and at low ^{35}S-activity (so as to be able to accurately monitor the ^{3}H-radioactivity from the C-terminal amino acid). The latter measurements showed that the weak 155-nucleotide band (lane 9, panel B) contained no tritium, demonstrating that only products shorter than the tetrapeptide were present in this case (cf. Table 1, below). Panels C and D show similar data from the peptides MK* and MK*FE, respectively. Here again, the 230-nucleotide band in lane 6 can be seen in the gel from the tetrapeptide (panel D), but not from the dipeptide (panel C). Otherwise the gels are very similar to those of panels A and B, with the notable exception that the 155-nucleotide band in lane 9) is very weak.

Table 2. Occurrence of cross-links I to V in the various peptides, summarized from the ribonuclease H data (cf. Figure 1).

Peptide	I (2062)	II (2506)	III (2585)	IV (2609)	V (1781)
M*	+	++	+	−	−
M*K	+	+	+	(+)	−
M*KF	+	(+)[a]	(+)[a]	+	(+)
M*KFE	+	(+)[a]	(+)[b]	+	+
MK*	++	(+)	(+)	(+)	−
MK*F	+	+	+	+	+
MK*FE	+	(+)	+	+	++

The deduced position of each cross-link in the 23S RNA sequence (cf. Figure 2) is given in parentheses. The symbols −, (+), + and ++ indicate that the cross-link concerned was absent, present in traces, clearly present, or strongly present, respectively. Each cross-linked peptide-23S RNA fragment complex was analysed for ^{3}H-radioactivity, as an indicator of the presence of the ^{3}H-labelled C-terminal amino acid in the peptide (see text and Table 1).

[a]Cross-linked band visible on ribonuclease H gel (cf. Figure 1, panel B), but with markedly reduced ^{3}H-radioactivity (Table 1).

[b]As for previous footnote, but with essentially zero ^{3}H-radioactivity (Table 1).

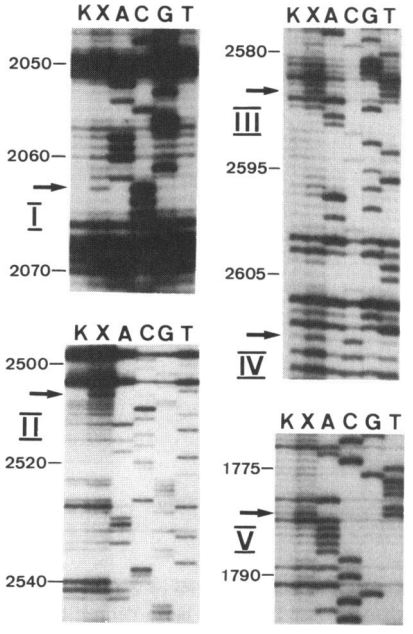

Figure 2. Primer extension analyses (20,11) of 23S RNA cross-linked complexes, corresponding to cross-links I to V. In each case lane K is a pre-irradiated control sample (see Materials and Methods), lane X is the cross-linked sample, and A, C, G, T are dideoxy sequencing lanes. Appropriate regions of the sequencing gels are shown, with the stop signals corresponding to cross-links I to V being indicated by the arrows. The substrates for the primer extension reactions shown were the cross-linked or control 23S RNA samples from the 'peptide' M* (for cross-links I, II), from the peptide M*KFE (cross-links III, IV), and from the peptide MK*FE (cross-link V). Oligodeoxynucleotide primers end-labelled with ^{32}P were used, complementary to 23S positions 2120–2139 (for cross-link I), 2649–2668 (for cross-links II, III, IV) and 1874–1893 (for cross-link V). (The strong stop signals at positions 2068, 2498 and 2503 are due to base modifications at these sites.)

Further ribonuclease H digestions were made in order to narrow down the 23S RNA regions encompassing the cross-link sites. Panel E (Figure 1) illustrates an example in which the cross-linked region from lane 6 (panel B) is progressively localized (digests 12 and 13) down to a 75-nucleotide region (between positions 1771 and 1845). These 'second round' digestions also serve to clarify occasional spurious cuts by the ribonuclease H (e.g. the band between the 390- and 155-nucleotide doublets in lane 9; such products arise from statistical partial complementarities of the oligodeoxynucleotides with other regions of the 23S RNA sequence). The final result of the ribonuclease H digestions was the localization of five distinct cross-linked 23S RNA regions, which we designate with Roman numerals as follows: I, positions 2054–2091 (a ca. 40-nucleotide stretch derived from the 270-nucleotide fragment in lane 7, Figure 1); II, positions 2460–2511 (a ca. 50-nucleotide stretch derived from the 155-nucleotide fragment in lane 9); III, positions 2572–2603, and IV, positions 2603–2623 (30- and 20-nucleotide stretches, respectively, resulting from a further resolution of the 110-nucleotide fragment from lane 10 into two cross-linked regions; data not shown); V, positions 1771–1812 (a ca. 40-nucleotide stretch derived from the 'new' cross-link in lane 6 in panels B and D, Figure 1). As noted above and in Materials and Methods, the radioactivity in the bands from the ribonuclease H gels was measured, so as to compare the contributions from the N-terminal ^{35}S-methionine and from the C-terminal ^{3}H-labelled amino acid. A typical analysis for each of the cross-linked 23S RNA regions I to V is given in Table 1, for the case of the tri- and tetrapeptides M*KF and M*KFE, respectively (cf. Table 2, below).

Further localizations of the cross-link sites within the 23S RNA regions I to V were made by the primer extension method (20,11), and typical examples of the reverse transcriptase gels obtained are illustrated in Figure 2. However, before describing this Figure, it is appropriate to briefly discuss the limitations of this technique in the analysis of cross-link sites. Whereas in a foot-printing type experiment (e.g. 22) the reverse transcriptase has to recognize a nick or modified nucleotide in a single RNA chain, in a cross-link analysis the bulky cross-linked ligand—in this case the tRNA—remains covalently attached to the RNA during the primer extension analysis. This has the consequence that the reverse transcriptase tends to 'stutter' as it approaches the cross-link site, as we (11) and other authors (23) have observed, thus making it difficult to pin-point the cross-link site precisely. Much more serious is the possibility that, during the annealing process with the primer, the RNA and cross-linked tRNA can form hybrid secondary or tertiary structures with one another, giving rise to additional pause or stop signals in the cross-linked sample lanes, which will be absent from the control lanes, but which are not cross-link sites. For this reason, we only regard a cross-link site as proven (10,11,31) if a reverse transcriptase stop signal is reproducibly observed within an RNA region that has already been unambiguously identified as closely as possible by the ribonuclease H tests using various combinations of oligodeoxynucleotides; spurious reverse transcriptase stop signals are not infrequently seen in our experiments outside the regions defined by the ribonuclease H, and in analyses which rely solely on the primer extension data—of which there are many examples in the literature (e.g. 24,25)—such signals would be interpreted as additional cross-link sites.

In the primer extension analyses shown in Figure 2, the assays were carried out on the total (cross-linked plus non-cross-linked) 23S RNA samples, as in ref. 11. It is therefore to be expected that reverse transcriptase stop signals at the cross-link sites are relatively weak, but nevertheless clear signals (which were also

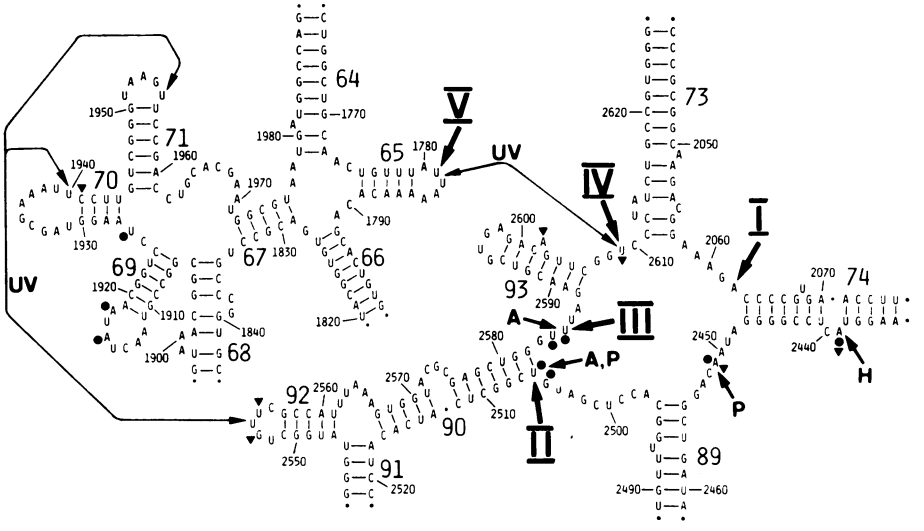

Figure 3. Part of the secondary structure of 23S RNA, showing the locations of cross-links I to V (compare with Table 1). The helices are numbered as in ref. 27, the 'peptidyl transferase ring' (28) being defined by the single-stranded regions connecting helices 73, 74, 89, 90 and 93. Intra-RNA cross-links induced by ultraviolet irradiation of 50S subunits (33) which connect the two secondary structural domains are indicated by the lines marked 'UV'. The cross-links observed by Steiner *et al.* (29) from affinity-labeled aminoacyl tRNA at the P- or A-site are denoted by 'P' or 'A' as appropriate, and a similar cross-link from aminoacyl tRNA derivatized with azido-hippuric acid at either the P- or A-site (11) is denoted by 'H'. The sites of foot-printing to tRNA at the P- or A-site described by Moazed and Noller (22,26) are indicated by the small filled circles and triangles, respectively. The naturally occurring modified bases in this region of the 23S RNA are not shown.

reproducible) can be seen within each of the five ribonuclease H regions. For cross-link I, in the ribonuclease H region between positions 2054 and 2091, stop signals occur in Figure 2 at nucleotides C-2063 and A-2062; [an additional problem in this region of the 23S RNA is the occurrence of massively strong stop signals caused by modified nucleotides or strong secondary and tertiary structures, also observed by other authors (e.g. 26)]. For cross-link II (ribonuclease H region 2460−2511) there is a stop signal at nucleotide C-2507. In the case of cross-links III and IV (ribonuclease H regions 2572−2603, and 2603−2623, respectively) some 'stuttering' can be seen, as just discussed, the most prominent stop signals being at nucleotides U-2585 and U-2586, and at C-2610. The 'new' cross-link V (ribonuclease H region 1771−1812) shows a single clear stop signal at nucleotide U-1782. On the basis of a large number of analyses similar to those depicted in Figure 2, and making the conventional assumption that each cross-link site is one base upstream from the most prominent and reproducible reverse transcriptase signal (see ref. 23 for a discussion of this point), the cross-link sites were assigned to 23S RNA positions 2062 (I), 2506 (II), 2585 (III), 2609 (IV) and 1781 (V). Interestingly, the cross-link sites I to V (if present at all) were always the same, regardless of the length of the peptide or the location of the diazirine label on methionine or lysine.

The complete set of data found in these experiments is summarized in Table 2, and the locations of the five cross-link sites in the secondary structure of the 23S RNA (27) are shown in Figure 3. Sites I to IV lie within the 'peptidyl transferase ring' (28), whereas site V is in a different secondary structural domain. In the series of peptides containing derivatized methionine (Table 2) there is a clear shift in the pattern of cross-linking as the peptide becomes longer; cross-links II and III show a marked reduction in intensity, whereas cross-link IV increases, and cross-link V is only seen in significant amounts with the tetrapeptide M*KFE, (although traces were visible in the tripeptide M*KF). Cross-link I on the other hand remains approximately constant, although as can be seen from Table 1 the full-length peptide was involved in this cross-link in both the tri- and tetrapeptides as well as in the 'mono'-peptide (Figure 1, panel A). Since the length of the diazirine reagent (ca 7 Å) is greater than the length of a single residue in the peptide chain (ca 4 Å), it is reasonable that the same cross-link sites can be reached from the N-termini of peptides of different lengths; the peptides themselves may of course also contribute to this flexibility. The corresponding pattern with the peptides carrying derivatized lysine (Table 2) shows a different quantitative distribution of the cross-links (I−IV) within the peptidyl transferase ring, and here cross-link V already appears with the peptide MK*F, which is effectively only a dipeptide with regard to the distance between the affinity-labelled and C-terminal amino acids. This result is consistent with the greater length and flexibility of the lysyl side-chain as compared to methionine. The appearance of cross-link V in both sets of peptides suggests that the peptides with the N-terminal diazirine group are following the same path as those with the natural N-formyl terminus; deviations may however become apparent at a future stage, with longer peptides.

Taken together with previous cross-linking data (11, 29, and cf. Figure 3) every one of the five single-stranded regions comprising the peptidyl transferase ring is now implicated as being close to or part of the peptidyl transferase centre itself. This is not trivial, since the ring consists of a total of 30 bases in single strands connecting five double-helices (Figure 3), which—fully extended—would represent a circumference of about 300 Å. The ring must therefore exist in a very compact configuration, and it is furthermore striking that the nucleotides involved in the cross-links coincide in several cases with those identified in tRNA foot-printing studies (22,26); the nucleotides concerned must in some way be particularly exposed. Cross-links

II and III also coincide with the sites found by Steiner *et al.* (29), who observed different patterns of cross-linking from an affinity-labelled aminoacyl residue, depending on whether it was located at the A or P site. However, this distinction was not corroborated by the tRNA foot-printing data (22); in particular the A site cross-link (29) was to nucleotides 2584–2585 (cf. Figure 3), positions which gave P site protection in the foot-printing studies (22). In our experiments, puromycin tests (data not shown) indicated a predominant P site binding (ca 80%) of the peptides, but—given that at the moment of peptidyl tranfer the aminoacyl or peptidyl residues in the A and P sites must be in direct contact—any distinction between the two sites on the basis of cross-linking data is not likely to be very informative. Rather, the results of Table 2 indicate that the peptide length must change by several residues before a significant change in the cross-linking pattern occurs.

In the context of our investigation, cross-link V to position 1781 of the 23S RNA is the most important observation, as this provides a first clear indication of the direction taken by the growing peptide as it leaves the peptidyl transferase centre. Previous data have defined a number of regions of the 23S RNA which must lie adjacent to the peptidyl transferase ring, and which could therefore be potential candidates for contacts with the exiting peptide. From intra-RNA cross-linking studies these regions include helices 35, 40 and 72 (30), or helix IV of the 5S RNA (31). Similarly, the region of helices 80–84 contains several cross-links to protein L27 (32), which has also been cross-linked to the aminoacyl residue of tRNA (e.g. 11). However, our data show that the exiting peptide is in fact directed towards helix 65 in domain IV of the 23S RNA, and it is noteworthy that nucleotides 1782 and 2609 (cf. cross-links IV and V) are among several pairs of nucleotides (Figure 3) which have been identified as connecting domain IV to the peptidyl transferase region in other direct intra-RNA cross-linking studies (33). We anticipate that the further application of our approach, in combination with refinements to the model which we have derived for the three-dimensional arrangement of the 23S RNA (33), will enable us to map the complete path of the nascent peptide through the 50S subunit, from the peptidyl transferase centre to the exit site. The location of cross-link V within helix 65 in our model of the 23S RNA (33) is consistent with the electron microscopic positioning (1,2) of the peptidyl transferase centre at the base of the central protuberance of the 50S subunit. On the other hand, our model (33) is only very preliminary in the region of the exit site (3) on the opposite side of the subunit, and therefore the question as to which parts of the 23S RNA sequence are likely to be located at or near the exit site remains open. However, preliminary experiments have already indicated that longer peptides finally 'break contact' with the peptidyl transferase ring altogether, and become successively cross-linked to sites within domain II and then domain I of the 23S RNA; these results will be presented in due course.

ACKNOWLEDGEMENTS

We thank Dr C.Gualerzi for the generous gift of initiation factors, and Drs K.H.Nierhaus and F.Triana for valuable discussions. The work was in part supported by a grant from the Deutsche Forschungsgemeinschaft (Br 632/3-1).

REFERENCES

1. Stöffler, G. and Stöffler-Meilicke, M. (1986) In Hardesty, B. and Kramer, G. (eds), *Structure, Function and Genetics of Ribosomes*. Springer Verlag, New York, pp. 28–46.
2. Oakes, M., Henderson, E., Scheinman, A., Clark, M. and Lake, J.A. (1986) In Hardesty, B. and Kramer, G. (eds), *Structure, Function and Genetics of Ribosomes*. Springer Verlag, New York, pp. 47–67.
3. Bernabeu, C. and Lake, J.A. (1982) *Proc. Natl. Acad. Sci. USA* 79, 3111–3115.
4. Yonath, A., Leonard, K.R. and Wittmann, H.G. (1987) *Science* 236, 813–816.
5. Ryabova, L.A., Selivanova, O.M., Baranov, V.I., Vasiliev, V.D. and Spirin, A.S. (1988) *FEBS Lett.* 226, 255–260.
6. Cantor, C.R., Pellegrini, M. and Oen, H. (1974) In Nomura, M., Tissières, A. and Lengyel, P. (eds), *Ribosomes*. Cold Spring Harbor Press, Cold Spring Harbor, New York, pp. 573–585.
7. Picking, W.D., Odom, O.W. and Hardesty, B. (1992) *Biochemistry* 31, 12565–12570.
8. Noller, H.F., Hoffarth, V. and Zimniak, L. (1992) *Science* 256, 1416–1419.
9. Stade, K., Rinke-Appel, J. and Brimacombe, R. (1989) *Nucleic Acids Res.* 17, 9889–9908.
10. Dontsova, O., Dokudovskaya, S., Kopylov, A., Bogdanov, A., Rinke-Appel, J., Jünke, N. and Brimacombe, R. (1992) *EMBO J.* 8, 3105–3116.
11. Mitchell, P., Stade, K., Osswald, M. and Brimacombe, R. (1993) *Nucleic Acids Res.* 21, 887–896.
12. Nassal, M. (1983) *Liebigs Ann. Chem.* 1983, 1510–1523.
13. Bochkariov, D.E. and Kogon, A.A. (1992) *Analyt. Biochem.* 204, 90–95.
14. Bochkareva, E.S., Lissin, N.M. and Girshovich, A.S. (1988) *Nature* 336, 254–257.
15. Wiedman, M., Kurzchalia, T.V., Hartmann, E. and Rapoport, T.A. (1987) *Nature* 328, 830–833.
16. Rheinberger, H.J., Geigenmüller, U., Wedde, M. and Nierhaus, K.H. (1988) *Methods Enzymol.* 164, 658–670.
17. Görlich, D., Kurzchalia, T.V., Wiedmann, M. and Rapoport, T.A. (1991) *Methods Cell Biol.* 34, 241–262.
18. Ehrenberg, M., Bilgin, N. and Kurland, C. (1990) In Spedding, G. (ed), *Ribosomes and Protein Synthesis; a Practical Approach*. IRL Press, Oxford, pp. 101–129.
19. Tate, W., Greuer, B. and Brimacombe, R. (1990) *Nucleic Acids Res.* 18, 6537–6544.
20. Moazed, D., Stern, S. and Noller, H.F. (1986) *J. Mol. Biol.* 187, 399–416.
21. Brunner, J., Senn, H. and Richards, F.M. (1980) *J. Biol. Chem.* 255, 3313–3318.
22. Moazed, D. and Noller, H.F. (1989) *Cell* 57, 585–597.
23. Denman, R., Colgen, J., Nurse, K. and Ofengand, J. (1988) *Nucleic Acids Res.* 16, 165–178.
24. Bhangu, R. and Wollenzien, P. (1992) *Biochemistry* 31, 5937–5944.
25. Nolan, J.M., Burke, D.H. and Pace, N.R. (1993) *Science* 261, 762–765.
26. Moazed, D. and Noller, H.F. (1991) *Proc. Natl. Acad. Sci.* USA 88, 3725–3728.
27. Brimacombe, R., Greuer, B., Mitchell, P., Osswald, M., Rinke-Appel, J., Schüler, D. and Stade, K. (1990) In Hill, W.E., Dahlberg, A.E., Garrett, R.A., Moore, P.B., Schlessinger, D. and Warner, J.R. (eds), *The Ribosome; Structure, Function and Evolution*. ASM Press, Washington DC, pp. 93–106.
28. Vester, B. and Garrett, R.A. (1988) *EMBO J.* 7, 3577–3587.
29. Steiner, G., Kuechler, E. and Barta, A. (1988) *EMBO J.* 7, 3949–3955.
30. Döring, T., Greuer, B. and Brimacombe, R. (1991) *Nucleic Acids Res.* 19, 3517–3524.
31. Dontsova, O., Tishkov, V., Dokudovskaya, S., Bogdanov, A., Döring, T., Rinke-Appel, J., Thamm, S., Greuer, B. and Brimacombe, R. (1994) *Proc. Natl. Acad. Sci. USA*, in press.
32. Brimacombe, R. (1991) *Biochimie* 73, 927–936.
33. Mitchell, P., Osswald, M., Schüler, D. and Brimacombe, R. (1990) *Nucleic Acids Res.* 18, 4325–4333.